Applied Physics Letters

Externally driven broadband transmission in strongly disordered materials

Cite as: Appl. Phys. Lett. **118**, 231103 (2021); https://doi.org/10.1063/5.0055926
Submitted: 04 May 2021 . Accepted: 11 May 2021 . Published Online: 10 June 2021

Nicolas Bachelard, Chad Ropp, Sui Yang, and Xiang Zhang

Applied Physics Letters ARTICLE scitation.org/journal/apl

Externally driven broadband transmission in strongly disordered materials

Cite as: Appl. Phys. Lett. **118**, 231103 (2021); doi: 10.1063/5.0055926
Submitted: 4 May 2021 · Accepted: 11 May 2021 ·
Published Online: 10 June 2021

Nicolas Bachelard,[1,2] Chad Ropp,[1] Sui Yang,[1,3] and Xiang Zhang[1,4,a)]

AFFILIATIONS

[1]NSF Nanoscale Science and Engineering Center, University of California, 94720 Berkeley, California, USA
[2]Institute for Theoretical Physics, Vienna University of Technology (TU Wien), A-1040 Vienna, Austria
[3]Materials Science and Engineering, School for Engineering of Matter, Transport and Energy, Arizona State University, Tempe, Arizona 85287, USA
[4]Faculty of Science and Faculty of Engineering, University of Hong Kong, Hong Kong, China

[a)]Author to whom correspondence should be addressed: xiang@berkeley.edu

ABSTRACT

In classical and quantum systems, order is of fundamental importance to many branches of science. Still, disorder is prevalent in our natural world. It manifests in various ways, and overcoming its limitations would open up exciting applications. In this work, we numerically show that disorder-induced Anderson localization can be mitigated and transmission systematically restored in random media through a self-organization process relying on energy dissipation. Under the scattering pressure produced by a driving optical field, a colloidal suspension composed of strongly polydisperse (i.e., random size) particles spontaneously assembles a Bloch-like mode with a broad transmission band. This mode displays a deterministic transmission scaling law that overcomes the statistical exponential decay expected in random media. This work demonstrates that, through the continuous dissipation of energy, amorphous materials can collectively synchronize with a coherent drive field and assemble a crystalline order. Self-organization, thus, offers a robust approach for addressing the physical limitations of disorder and immediately opens the door to applications in slow-light engineering and the development of "bottom-up" photonic materials.

The effects of disorder are pernicious in science and often hinder technological progresses. In both organic[1] and inorganic[2] condensed matter, the effects of imperfections manifest at different scales,[3] often limiting electron mobility,[4] and, in extreme cases, cause material phase transitions.[5,6] In the quantum world, disorder severely impacts the properties of quantum gases[7] and prevents many-body systems from reaching thermal equilibrium (e.g., in many-body localization[8]). Disorder also remains an increasing concern in photonics. With the progressive convergence toward nanoscale dimensions, nanophotonic technologies become fundamentally limited by fabrication imperfections, which are inherent to both "top-down"[9] and bottom-up processes[10] alike. Imperfections introduce both scattering losses—energy lost through radiation to the surroundings—and backscattering effects—coherent perturbation of the forward-propagating wave-front. The later effect ultimately leads to unwanted random-interference-based spatial confinement, known as Anderson localization.[6,11] Backscattering stands as the major limitation for the realization of high-group-index structures, such as slow-light waveguides[12,13] and resonant optical nanocavities,[14,15] which would require fabrication precisions better than state-of-the-art top-down technologies can overcome.[16,17] The challenge of mitigating disorder has led to the development of post-fabrication correction schemes (e.g., through thermal[18] or electrical[19] tuning), which are difficult to scale to architectures with many components. Alternatively, different mechanisms, such as topology[20] or cascaded locking,[21] have been explored to suppress the impact of disorder. Yet, these approaches come at the price of either breaking time-reversal symmetry (e.g., through the application of strong magnetic fields) or strong optical nonlinearities, which are both difficult to achieve at optical frequencies.

Self-organization defines a class of bottom-up processes enabling the assembly of massive numbers of nanoscale particles to fabricate low-cost devices. The most common approach among such technologies is self-assembly—in which, elements are led to relax (e.g., through a chemical reaction) toward an ordered equilibrium state.[22] While self-assembly has been proposed to fabricate components like color displays[23] or solar-cells,[24] it is not immune to the effects of disorder.

A major concern is element polydispersity, for which stable large-scale structures often require size dispersions below a few percent.[25] In contrast to the self-assembly of equilibrium structures, dissipative self-organization of non-equilibrium structures is an alternative bottom-up approach, occurring when structures are driven to organize through the coordinated and constant dissipation of energy.[22] This mechanism is common in nature, giving rise to dynamic structures and behaviors, such as collective flocking in both schools of fish and swarms of fireflies.[26,27] Dissipative self-organization has found many analogues in artificial living systems[28] and has recently been reported to form self-healing and self-adaptive bandgap crystals.[29,30] At the macro-scale, the reproduction of this process is led to the formation of non-equilibrium structures similar to animal flocks,[31] which often display a unique robustness to element heterogeneity (i.e., size dispersion),[32] external perturbation,[29] and environmental disorder.[33] Yet, dissipative self-organization has never been envisioned to mitigate the impact of imperfections in the manufacturing of bottom-up devices.

In this Letter, we numerically demonstrate that strongly disordered media, governed by Anderson localization, can systematically assemble crystal-like order. A colloidal suspension of polydisperse nanoparticles self-organizes to form Bloch-like modes when driven by the radiation forces exerted by a monochromatic scattered field. Independently of disorder strength, an anomalous transmission response emerges following a universal scaling law unexpected for random media. This disorder-protected mode is characterized by a spatially asymmetric profile and a non-Lorentzian group-index resonance that strengthens linearly with the number of particles. Dissipative self-organization is shown to be mechanically robust and reliably reproducible in media with size dispersion greater than an order of magnitude. These results demonstrate that coherently driven self-organization could enable the enhancement of broadband transmission and slow-light characteristics in disordered structures.

The self-organization of an ensemble of N random-sized Rayleigh scatterers is simulated using a transfer matrix formalism (supplementary material). The particles are assumed to be made of zinc-oxide and are viscously damped in a background solution while being constrained to move in one dimension along a single-mode waveguide [Fig. 1(a)]. The diameter of the nth particle, D_n, follows a Gaussian distribution with a varied dispersion σ and mean $\overline{D} = 100\,\text{nm}$. The size dispersion results in an inhomogeneity in the reflection coefficients, R_n. We numerically simulate the action of an incident monochromatic drive of wavelength $\lambda_0 = 1.5\,\mu\text{m}$. The drive is collectively scattered, and its momentum is transferred to the particles through optical forces, F_n, which depend on the difference in intensity across each particle. Starting from random initial spacings ($t = 0$), the particles spontaneously converge toward a steady state ($t = t_{ss}$) where they move at identical speeds and their spacings remain constant over time (supplementary material Fig. S1). At steady state, the kinetic energy is constantly balanced with the dissipation of viscous friction and a uniform force distribution is reached, which corresponds to the momentum being equally shared among elements—i.e., $F_n = F_S = \frac{2(1-T_S)}{N}\,\forall\, n$ (in which the steady-state total transmission, T_S, is analytically derived in the supplementary material). For small-dimensions scatterers, we observe that the particles redistribute within the optical field close to maxima of field intensity (supplementary material Fig. S2).

Despite strong initial disorder, dissipative self-organization systematically produces steady states with anomalous and spectrally broad transmission windows [two distinct examples provided in Fig. 1(b)]. Before the drive is turned on, the transmission spectra display many Anderson-localized modes (peaks in blue curves), which are signatures of the strong disorder present in the random medium.[34] During the self-organization, the particles move and, thus, dynamically reshape the optical states—pushing modes out to form a bandgap[29] and merging modes to create the transmission window. The final steady-state transmission spectra (orange curves) are characterized by a continuous transmission band of width $\Delta\lambda \approx 350\,\text{nm}$ for $N = 50$ and with close-to-100% maximum transmission. Such transmission response is reproduced over multiple disorder configurations for increasing population sizes, N, and different size dispersions, σ [Fig. 1(c) and inset, respectively]. The spectral width slowly reduces with the number of particles, N, and appears robust against large disorder strength σ (inset).

The emerging order also displays an intrinsic protection against parametric perturbations [Fig. 1(d)]. A steady state is organized out of a population of $N = 50$ particles, and at a specific time (red star), the index of refraction of each element is randomly changed (modification of 25%, supplementary material). Despite this major perturbation across the whole system, a stable steady state with similar properties reforms, thus emphasizing an intrinsic and dynamic protection against disorder.

While transmission channels in strongly disordered media are governed by randomly distributed Anderson-localized modes,[35] here, the broadband response self-organizes into a deterministic distribution resembling a Bloch mode—regardless of the degree of disorder. This self-organization is driven by a synchronization of the phase of the driving field. Starting at $t = 0$, the initial phase distributions of the polydisperse particles sets are utterly random (supplementary material Fig. S3); however, after self-organization the steady-state phase distribution, $\Phi_B(n)$ [inset Fig. 1(a)], systematically approaches a uniform distribution with element-to-element phase differences held close to π [black, dark, and light blue curves in Fig. 2(a)]. At the far end of the structure, $\Phi_B(n)$ deviates from π due to the open-boundary condition. This nearly uniform π-phase distribution resembles that of a Bloch mode in a periodic medium, which, like in photonic crystals, is associated with a band edge mode with a bandgap at lower wavelengths and a transmission band at longer wavelengths (supplementary material Fig. S4 and discussion therein). Our steady-state phase distribution is enforced by the mechanical steady-state condition, which requires identical forces on individual particles (i.e., $F_1 = \cdots = F_N = F_S$). Therefore, $\Phi_B(n)$ is ensured to be close to π regardless of the distribution of particle sizes. Using the mean particle reflectivity $\overline{R}$, in the supplementary material, an approximation-free analytical expression for the mean phase distribution is derived and reads $\overline{\Phi}_B(n) = \pi - \delta(n)$, where

$$\delta(n) = \frac{1}{2}\text{asin}\left(\sqrt{\frac{1+(N-n)\overline{R}}{1+N-n}}\right) + \frac{1}{2}\text{asin}\left(\overline{R}\sqrt{\frac{1+N-n}{1+(N-n)\overline{R}}}\right) - \text{acos}\left(\sqrt{\frac{(1-\overline{R})\left(1+(N-n+1)\overline{R}\right)}{1+(N-n)\overline{R}}}\right). \quad (1)$$

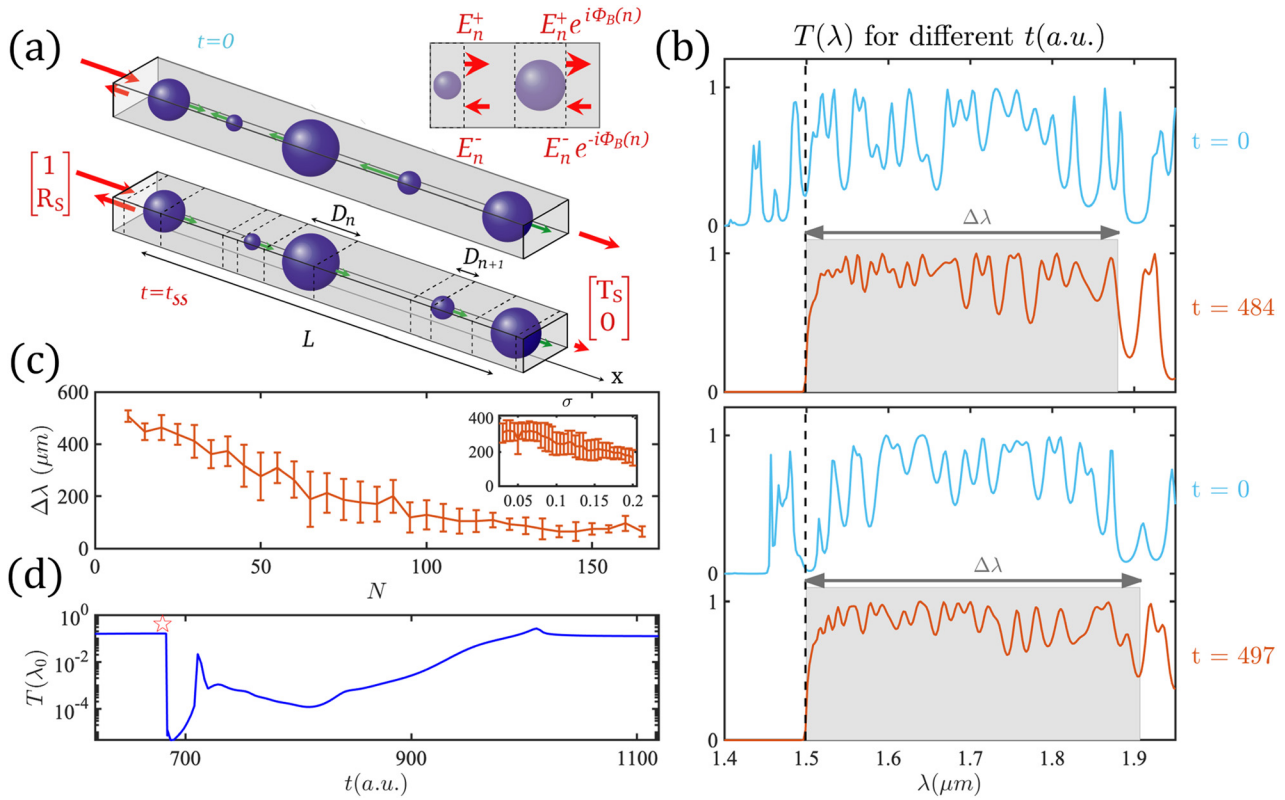

FIG. 1. Emergent transmission within a polydisperse random medium through dissipative self-organization. (a) Schematic of system geometry and self-organization. An array of randomly sized nanoparticles begins randomly distributed along a 1D optical waveguide ($t = 0$, top diagram). A coherent drive (red arrows) is inserted from the left end. The field scatters among the particles causing them to move (green arrows). The system reaches a steady-state configuration ($t = t_{SS}$, bottom diagram), in which the particles are mechanically stable and move collectively away from the source (orange arrows). Inset: from the $(n-1)$th to the nth particles the forward component of the field E_n^+ accumulates a phase $\Phi_B(n)$, while a phase of $-\Phi_B(n)$ is accumulated on the backward component E_n^-. (b) Two transmission spectra (blue) corresponding to two distinct initial arrangements of $N = 50$ particles with a dispersion of $\sigma = 5\%$. The steady-state spectra obtained after self-organization are plotted in orange with the full-width-half-maximum $\Delta\lambda$ transmission window labeled in gray. (c) Width of the transmission window as a function of the number of particles within the ensemble. Data shows the average and standard deviation from 10 simulations corresponding to different initial particles sets. The transmission window $\Delta\lambda$ decreases with the addition of more particles, yet it appears robust against large particle dispersion σ (inset). (d) Transmission at drive wavelength, $T(\lambda_0)$, as a function of time for a system of $N = 50$ particles. The system is first self-organized ($t < 680$). Then, at $t = 680$ (red star), the indices of refraction are randomly modified and the system dynamically reconfigures to re-form a high-transmission steady state ($t > 1050$).

Importantly, $\overline{\Phi}_B(n)$ does not depend on the polydispersity σ and perfectly matches our numerical calculations [red curves in Fig. 2(a)]. Larger dispersions show larger variations about $\overline{\Phi}_B(n)$ [black, dark, and light blue error bars in Fig. 2(a)]; however, the mean response holds true so long as the mechanical steady-state condition is met. The influence of open-boundary condition at the right-end side can also be observed in the spatial distribution of particles within the optical field [supplementary material Fig. S2].

The universality of the steady-state phase distribution causes the transmission of the drive to similarly follow a deterministic and universal scaling law that is independent of disorder strength. Figure 2(b) displays the mean transmission at λ_0, $\overline{T}(\lambda_0)$, as a function of system size L (obtained by increasing the number of particles, N) and under the different dispersion used in Fig. 2(a). Before self-organization, and as expected for random media, the systems decay as $\overline{T}(\lambda_0) \propto \exp(-L/\xi_\sigma)$, in which ξ_σ stands for the localization length (identical to the scattering length in 1D systems[7]) After self-organization, the mean transmissions systematically collapse onto a singular curve (inset zoom), which follows a non-exponential scaling law ($\overline{T}_S(\lambda_0) \propto 1/L$). Remarkably, this emergent trend is deterministic and independent of disorder strength, σ, appearing in both weakly disordered systems (i.e., $L < \xi_\sigma$) and strongly disordered systems governed by Anderson localization (i.e., $L > \xi_\sigma$). An analytic expression for the mean transmission across the ensemble can be found in the supplementary material and reads

$$\overline{T}_S(\lambda_0) = \frac{1-\overline{R}}{1+\overline{R}(N-1)}, \tag{2}$$

which is red plotted in Fig. 2(b) and matches our numerical results. This inverse-linear (i.e., $1/L$) trend ensures that, regardless of disorder strength, transmission will be restored for long structures compared to typical un-organized exponential decay.

In addition to the restoration of transmission, the self-organized system assembles a slow-light resonance at λ_0. The formation of resonances has been reported in other macro-scale periodically driven

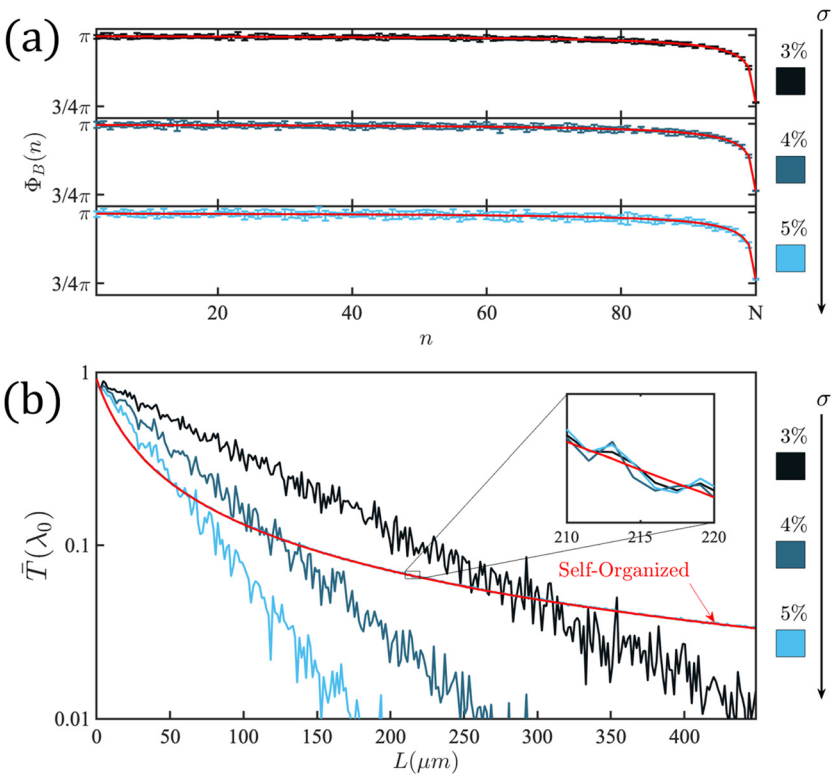

FIG. 2. Universal response of the self-organized system. (a) Curves of the phase accumulated, $\Phi_B(n)$, at λ_0 by the forward propagating field in the self-organized system between successive particles along the structure—i.e., from the $(n-1)$th and nth element [inset of Fig. 1(a)]. The three different curves show the phase distribution for $\sigma = 3\%$, 4%, and 5% (black to light blue) averaged over 10 simulations. All data fall onto the same analytic mean steady-state phase distribution, $\overline{\Phi}_B(n)$ [red lines, Eq. (1)]. (b) Trend for the transmission at λ_0 as a function of the length of the structure for $\sigma = 3\%$, 4%, and 5% (black to light blue). Before self-organization, the trends decay exponentially. After self-organization, all curves fall onto the single analytical trend, $\overline{T}_S(\lambda_0)$, provided in Eq. (2) (red curve with inset zoom highlighting the collapse to the trend line).

self-organized systems.[36] Here, this feature materializes through the emergence in the transmission spectrum of a band edge at λ_0 [Fig. 3(a)]. The emerging band edge defines a resonance in the density of optical states[37] that one can observe in the group-index spectra, $n_g(\lambda)$, displayed in Fig. 3(b). The amplitude of the resonance, $n_g(\lambda_0)$, is shown to increase linearly with the addition of more particles [inset Fig. 3(b)], which relates to the stiffening of the band edge when increasing N [Fig. 3(a)]. Remarkably, the observed group-index resonances appear with an unusual asymmetric shape. Such resonances describe a kind of modes that fundamentally differs from conventional slow-light modes reported in both photonic crystals[37] and Anderson-localized systems,[34] which typically exhibit symmetric Lorentzian profiles. The origin of such asymmetry is revealed by the spatial distribution of drive field intensity [Fig. 3(c)]. Rather than being exponentially decaying or exponentially localized—as expected in random media, here the field intensity progressively decays and extends across the full length of the structure. In the supplementary material, we show that the self-organization of the optical field at steady state provides spatial-correlation properties similar to ideal crystals (supplementary material Fig. S5).

The observed self-organization is remarkably robust to very inhomogeneous sets of particles with up to a factor 10 in size dispersion. While conventional bottom-up approaches like self-assembly typically require highly monodispersed particles ($\sigma = 3\%$ in Ref. 38) this approach demonstrates an ability to assemble strongly polydisperse elements. To analytically estimate the tolerances in size dispersion, we first consider that the mechanical steady state holds only when the momentum of the drive field is uniformly distributed among elements—which reads $F_n = F_S \,\forall\, n$. This transfer of momentum varies with particles' sizes. Thus, for extreme size dispersion, the existence of small or large particles might prevent the formation of a mechanically stable steady state and lead to collisions. The requirement of stability places a restriction on the reflection coefficients of individual particles, R_n, which we find must be constrained within boundaries solely imposed by the reflectivity of the last particle, R_N (supplementary material). This restriction reads

$$(\Delta R_n^- + R_N) < R_n < (\Delta R_n^+ + R_N) \forall\, n \in [1, N], \tag{3}$$

in which

$$\frac{\Delta R_n^{\pm}}{R_N} = \frac{2(\mathrm{N}-\mathrm{n})(1+\mathrm{R_N}(\mathrm{N}-\mathrm{n}))}{(2R_N(N-n)+1)^2} \times \left(1 - 2\mathrm{R_N} \pm \sqrt{\frac{(1+N-n)(1+R_N(N-n-1))}{(\mathrm{N}-\mathrm{n})(1+\mathrm{R_N}(\mathrm{N}-\mathrm{n}))}}\right). \tag{4}$$

An example of the stability condition derived from Eq. (4) is plotted in Fig. 4(a). Equation (3) applies independently to each particle, as numerically confirmed in Fig. 4(b). The stability condition is imposed by the second-to-last or $(N-1)$th particle [Fig. 4(a)], from which we obtain the reflection coefficient range $[R_{min}, R_{max}] \approx \left[\frac{R_N}{6}, 6R_N\right]$ that reveals independent of N. Translated into an equivalent diameter [supplementary material Fig. S6(a)], the stability range for a system with an average diameter of $\overline{D} = 100\,\mathrm{nm}$ must have individual

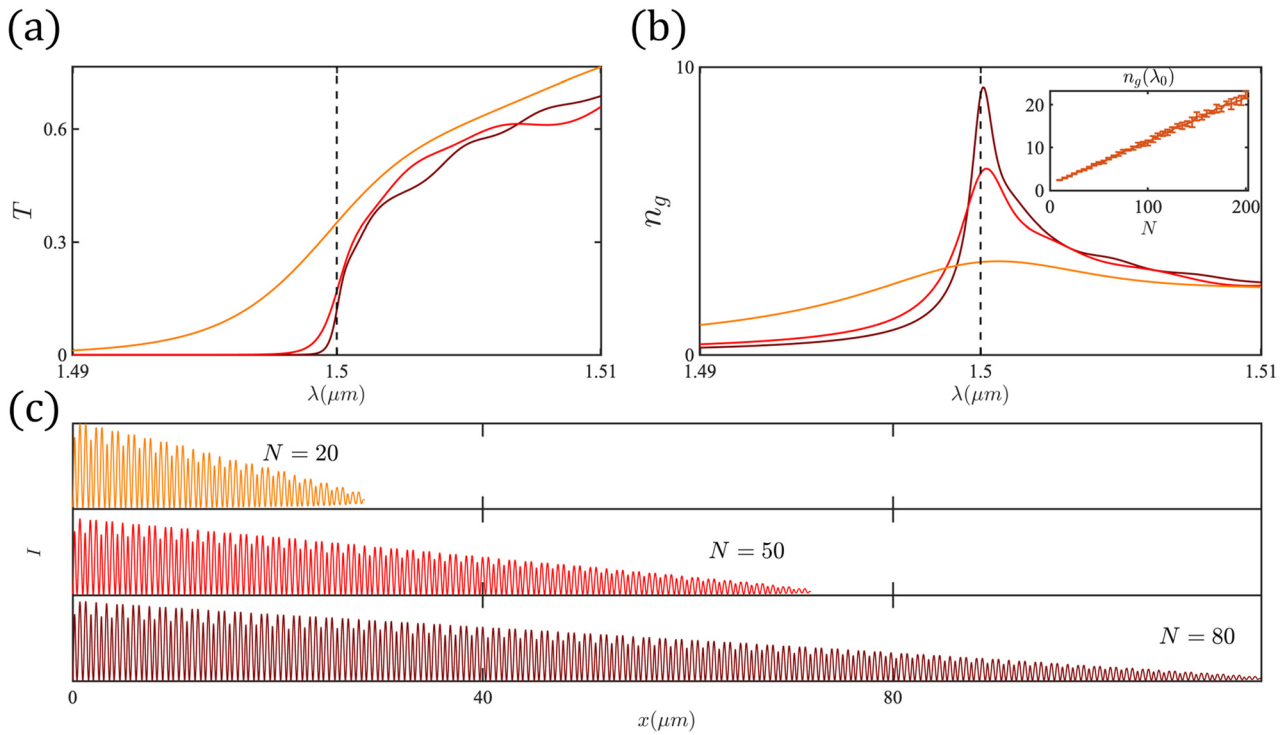

FIG. 3. Emergence of slow-light resonances through self-organization. (a) Transmission spectra near λ_0 for three different system lengths ($N = 20$, 50, and 80 particles; curves are orange, red, and dark red, respectively) and $\sigma = 5\%$. (b) Group-index spectra near λ_0 for the three systems of (a). The inset shows the linear increase in the group index at λ_0 as a function of the number of particles (data taken over 10 different random configurations). (c) Spatial profiles of the self-organized mode at λ_0 for the three different structures used in panels (a) and (b). In each case, the field extends over the entire length of the structure and shows a progressively linear decay away from the source (located at $x = 0$).

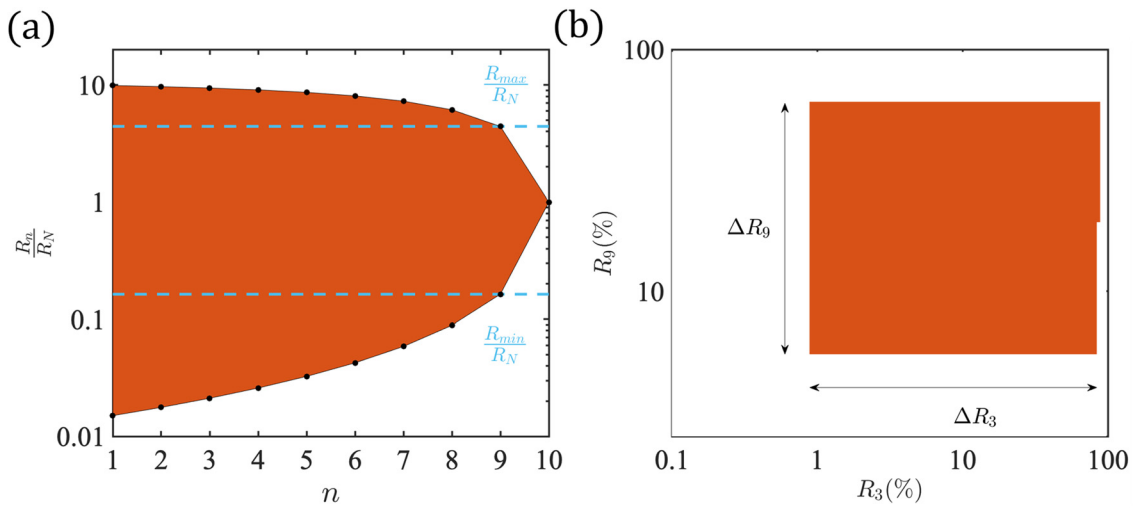

FIG. 4. Robustness of self-organization against particles dispersion. (a) For $N = 10$ particles with $R_N = 8.82\%$, the ensemble self-assembles if each individual reflection coefficients, R_n, lay within the stability boundaries of Eqs. (3) and (4) (orange region). The smallest stability range is indicated by the dashed blue lines and is imposed by the second-to-last particle. **(b)** Numeric confirmation of the analytic expression of Eqs. (3) and (4) for a set of $N = 10$ with $\sigma = 5\%$, in which the reflection coefficients of the $n = 3$rd and $n = 9$ th particles are varied by changing their refractive indices. The orange (respectively, white) region corresponds to the stability (respectively, instability) domain, in which the system self-organizes (respectively, collapses). The sizes of the stability domains (ΔR_3, ΔR_9) correspond to the theoretical prediction of Eq. (4).

diameters restricted to 34 nm $\leq D_n \leq$ 340 nm. supplementary material Figs. S6(b) and S6(c) display self-organization examples for large size dispersion ($\sigma = 20\%$).

In this work, we demonstrated that highly disordered materials can be driven to self-organize into a well-protected ordered photonic structure. Our system spontaneously synchronizes the drive phase to form Bloch-like modes through coherent momentum sharing among elements. The transmission of these modes is governed by a deterministic scaling law, which exceeds the exponential decay expected in random media and is revealed to be independent of disorder strength. Simultaneously, we showed that the system assembles a group-index resonance (i.e., slow-light mode) that strengthens with system size. The self-organization process is robust over large particle dispersions and could be integrated with photonic technologies to create scalable photonic devices and mitigate the effects of disorder in general and backscattering in particular. Thus, our results introduce a pathway for the conception of backscattering-free slow-light devices with performances only limited by scattering losses. While state-of-the-art slow-light structures are mainly limited by backscattering (scaling as n_g^2),[39] such devices could potentially reach orders-of-magnitude-higher group indices (scattering losses only scaling as n_g). Finally, although this work focused on the self-organization through particle motion, recent works suggest that similar responses can be replicated in solid-state platforms,[30] which highlights that dissipative self-organization could be readily extended to other branches of physics and condensed matter systems.

See the supplementary material for the numerical procedure followed to observe self-organization and the analytical derivations of Eqs. (1)–(4) are described in the supplementary material. There, we also discuss the formation of a crystal-like organization at steady state and provide all the supplementary figures mentioned throughout the text.

The work is supported by the King Abdullah University of Science and Technology Office of Sponsored Research (OSR) (Award No. OSR-2016-CRG5-2950-03). The contribution from Nicolas Bachelard was supported by the European Union through the Horizon 2020 research and innovation program under the Marie Skłodowska-Curie Grant Agreement No. 840745 (ONTOP).

DATA AVAILABILITY

The data that support the findings of this study are available from the corresponding author upon reasonable request.

REFERENCES

[1]H. Sirringhaus, Adv. Mater. **26**, 1319 (2014).
[2]J. Yang and F. W. Wise, J. Phys. Chem. C **119**, 3338 (2015).
[3]D. P. McMahon and A. Troisi, ChemPhysChem **11**, 2067 (2010).
[4]R. Noriega, J. Rivnay, K. Vandewal, F. P. V. Koch, N. Stingelin, P. Smith, M. F. Toney, and A. Salleo, Nat. Mater. **12**, 1038 (2013).
[5]M. Imada, A. Fujimori, and Y. Tokura, Rev. Mod. Phys. **70**, 1039 (1998).
[6]A. Lagendijk, B. van Tiggelen, and D. S. Wiersma, Phys. Today **62**(8), 24 (2009).
[7]L. Sanchez-Palencia and M. Lewenstein, Nat. Phys. **6**, 87 (2010).
[8]R. Nandkishore and D. A. Huse, Annu. Rev. Condens. Matter Phys. **6**, 15 (2015).
[9]L. Sapienza, H. Thyrrestrup, S. Stobbe, P. D. Garcia, S. Smolka, and P. Lodahl, Science **327**, 1352 (2010).
[10]A. Maity, S. Mujumdar, and V. Polshettiwar, ACS Appl. Mater. Interfaces **10**, 23392 (2018).
[11]P. W. Anderson, Phys. Rev. **109**, 1492 (1958).
[12]B. Wang, S. Mazoyer, J. P. Hugonin, and P. Lalanne, Phys. Rev. B **78**, 24518 (2008).
[13]S. Mazoyer, J. P. Hugonin, and P. Lalanne, Phys. Rev. Lett. **103**, 063903 (2009).
[14]S. Mookherjea, J. S. Park, S.-H. Yang, and P. R. Bandaru, Nat. Photonics **2**, 90 (2008).
[15]E. Gil-Santos, C. Baker, A. Lemaître, C. Gomez, G. Leo, and I. Favero, Nat. Commun. **8**, 14267 (2017).
[16]J. Liang, L. Y. Ren, M. J. Yun, X. Han, and X. J. Wang, J. Appl. Phys. **110**, 2 (2011).
[17]Y. Zhao, Y. N. Zhang, Q. Wang, and H. Hu, IEEE Trans. Nanotechnol. **14**, 407 (2015).
[18]P. Dong, W. Qian, H. Liang, R. Shafiiha, D. Feng, G. Li, J. E. Cunningham, A. V. Krishnamoorthy, and M. Asghari, Opt. Express **18**, 20298 (2010).
[19]Y. Shen, I. B. Divliansky, D. N. Basov, and S. Mookherjea, Opt. Lett. **36**, 2668 (2011).
[20]M. Hafezi, E. A. Demler, M. D. Lukin, and J. M. Taylor, Nat. Phys. **7**, 907 (2011).
[21]E. Gil-Santos, M. Labousse, C. Baker, A. Goetschy, W. Hease, C. Gomez, A. Lemaître, G. Leo, C. Ciuti, and I. Favero, Phys. Rev. Lett. **118**, 063605 (2017).
[22]M. Fialkowski, K. J. M. Bishop, R. Klajn, S. K. Smoukov, C. J. Campbell, and B. A. Grzybowski, J. Phys. Chem. B **110**, 2482 (2006).
[23]S. H. Kim, S. Y. Lee, S. M. Yang, and G. R. Yi, NPG Asia Mater. **3**, 25 (2011).
[24]M. A. Boles, M. Engel, and D. V. Talapin, Chem. Rev. **116**, 11220 (2016).
[25]C. B. Murray, C. R. Kagan, and M. G. Bawendi, Annu. Rev. Mater. Sci. **30**, 545 (2000).
[26]R. E. Mirollo and S. H. Strogatz, SIAM J. Appl. Math. **50**, 1645 (1990).
[27]N. Shimoyama, K. Sugawara, T. Mizuguchi, Y. Hayakawa, and M. Sano, Phys. Rev. Lett. **76**, 3870 (1996).
[28]A. Bricard, J.-B. Caussin, N. Desreumaux, O. Dauchot, and D. Bartolo, Nature **503**, 95 (2013).
[29]N. Bachelard, C. Ropp, M. Dubois, R. Zhao, Y. Wang, and X. Zhang, Nat. Mater. **16**, 808 (2017).
[30]C. Ropp, N. Bachelard, D. Barth, Y. Wang, and X. Zhang, Nat. Photonics **12**, 739 (2018).
[31]Q. Chen, P. Torroni, S. Villata, J. Hsu, and R. Goebel, *PRIMA 2015: Principles and Practice of Multi-Agent Systems* (Springer International Publishing, Cham, 2015).
[32]G. M. Whitesides, B. A. Grzybowski, and H. A. Stone, Nature **405**, 1033 (2000).
[33]A. Morin, N. Desreumaux, J.-B. Caussin, and D. Bartolo, Nat. Phys. **13**, 63–67 (2017).
[34]A. Cazé, R. Pierrat, and R. Carminati, Phys. Rev. Lett. **111**, 053901 (2013).
[35]A. Peña, A. Girschik, F. Libisch, S. Rotter, and A. A. Chabanov, Nat. Commun. **5**, 3488 (2014).
[36]T. Kachman, J. A. Owen, and J. L. England, Phys. Rev. Lett. **119**, 038001 (2017).
[37]A. Yariv and P. Yeh, *Photonics: Optical Electronics in Modern Communications* (Oxford University Press, New York, 2007).
[38]I. G. Denisov, Y. V. Grinkova, A. A. Lazarides, and S. G. Sligar, J. Am. Chem. Soc. **126**, 3477 (2004).
[39]P. Lalanne, S. Coudert, G. Duchateau, *et al.*, ACS photonics **6**(1), 4–17 (2018).